Available online at www.sciencedirect.com
ScienceDirect
Polymer 47 (2006) 7726–7730
polymer
www.elsevier.com/locate/polymer

Effect of sample size on Case II diffusion of methanol in poly(methyl methacrylate) beads

Jian-Xin Li[1], Ping I. Lee*

Department of Pharmaceutical Sciences, Faculty of Pharmacy, University of Toronto, 19 Russell Street, Toronto, Ontario M5S 2S2, Canada

Received 12 April 2006; received in revised form 29 August 2006; accepted 30 August 2006
Available online 22 September 2006

Abstract

The effect of sample size on the characteristic Case II solvent front penetration behavior has been investigated in a methanol–PMMA bead system at 25 °C in the particle diameter range of 0.125–1.280 mm. The observed induction time generally increases, whereas the front penetration rate exhibits a weak decreasing trend, with increasing sample diameter. Such dependencies of induction time and front penetration rate on sample size, although not predicted by existing theories of Case II diffusion, can be attributed to the size-dependent nature of several physical processes originated from the Fickian precursor penetrating ahead of the moving solvent front in an inhomogeneous swelling system of finite dimension.

Keywords: Case II diffusion; Sample size effect; PMMA beads

1. Introduction

The diffusion of small molecule solvents in glassy polymers is known to exhibit Case II behavior [1]. This is characterized by the existence of: (1) a sharp solvent front in the polymer advancing at a constant velocity (or linear weight-gain kinetics), (2) a negligible solvent concentration gradient behind the sharp solvent front, and (3) an induction time leading to the onset of front movement. Such non-Fickian sorption process has been investigated extensively over the past four decades. For example, Thomas and Windle [2–4] studied these characteristic features of Case II diffusion during methanol sorption in glassy poly(methyl methacrylate) (PMMA) and modeled such Case II diffusion process in terms of the viscous response of polymer glass to the osmotic swelling pressure generated by the penetrating solvent. Hui et al. [5–7] refined Thomas and Windle's mechanistic model and employed Rutherford backscattering spectrometry for the determination of penetrant concentration profiles in the polystyrene/iodohexane system. Their results appear to verify the existence of various essential features of Case II diffusion as predicted by the model of Thomas and Windle, particularly the Fickian precursor ahead of the sharp solvent front and the induction period before establishing a constant rate of front movement. In addition, their results clearly demonstrate that the initiation of Case II front movement can only take place after a critical volume fraction of penetrant has been reached at the surface of the glassy polymer, after which the polymer viscosity would be lowered sufficiently and the diffusion coefficient of the penetrant increased to the level necessary for establishing the Case II front [7]. In other words, the surface volume fraction of the penetrant does not immediately reach this critical value after the first exposure of a glassy polymer sample to solvent, hence the existence of an induction time. This physical consideration is also consistent with the phenomenological description of Case II diffusion proposed by Rossi et al. [8], which is based on the concept of plasticization at a sufficiently high solvent concentration where the slow plasticization kinetics sets an upper limit for the solvent flux into the glassy region.

* Corresponding author. Tel.: +1 416 946 0606; fax: +1 416 978 8511.
E-mail address: ping.lee@utoronto.ca (P.I. Lee).
[1] Present address: FMC BioPolymers, US Route 1 and Plainsboro Road, Princeton, NJ 08543, USA.

0032-3861/$ - see front matter © 2006 Elsevier Ltd. All rights reserved.
doi:10.1016/j.polymer.2006.08.065

Since most of the experiments documenting Case II diffusion were based on sheet specimens, the role of sample geometry on penetrating solvent front movement and the effect of sample size on Case II behavior were largely overlooked for quite some time as a result. In regards to the former, Lee et al. [9,10] presented theoretical and experimental results comparing the penetrating front movement in sheet and spherical bead samples of identical glassy polymers, thus resolving the fundamental issue regarding the geometry-dependent Case II behavior. It was demonstrated that only the initial stage of the constant-rate front penetration behavior is independent of sample geometry. The later stage of front penetration exhibits an apparent acceleration of solvent front towards the core in spheres and cylinders, which has been shown to be a natural outcome of the radially symmetric sample geometry rather than a Super Case II behavior as suggested by some previous authors.

On the other hand, the effect of sample size on Case II diffusion behavior has not been reported. Historically, the induction time and constant front penetration rate have long been regarded as material properties of the glassy polymer for a given penetrant [2–8,11], as such they are generally treated as independent of sample size and geometry. Again, since experiments documenting Case II diffusion were mostly based on sheet specimens and existing theories of Case II diffusion were developed accordingly only for semi-infinite one-dimensional systems, it is not surprising that none of these existing theories is capable of predicting the dependence of induction time and front penetration rate on sample dimension in radially symmetric geometries.

In this study, we report for the first time evidence showing sample size-dependent induction time and front penetration rate during Case II diffusion of methanol in glassy spherical PMMA beads. Underlying reasons for such observed size dependencies are proposed based on the consideration of physical processes occurring due to the presence of a Fickian precursor ahead of the moving front in a three-dimensional inhomogeneous swelling system of finite dimension. These include the time requirement for PMMA beads to reach the threshold methanol concentration at the surface prior to establishing the moving front, as well as the presence of compressive surface stress in partially swollen PMMA beads and the known dependence of Case II diffusion behavior on applied stress.

2. Experimental

2.1. Synthesis of polymer beads

The synthesis of spherical PMMA beads and their purification in methanol have been described in details elsewhere [10]. Briefly, PMMA beads were prepared by free radical suspension polymerization of freshly distilled methyl methacrylate at 70 °C for 3 h using *t*-butyl peroxy-2-ethylhexanoate as the initiator and freshly precipitated $Mg(OH)_2$ as the suspending agent. After completion of polymerization, concentrated HCl was added to remove the suspending agent. The beads obtained were filtered and Soxhlet extracted with methanol before being dried to a constant weight in a vacuum oven, typically at 70–80 °C for 3–5 days. Based on the intrinsic viscosity measurement in acetone obtained on a Ubbelohde viscometer, the average molecular weight of the PMMA beads was estimated to be about 5.2×10^5 from the Mark–Houwink equation. PMMA beads in the diameter range of 0.125–1.280 mm were used in the present study. Prior to the swelling experiment, these beads were annealed at 130 °C for 3 h under nitrogen and subsequently cooled to room temperature at different programmed rates on a Perkin–Elmer DSC to relieve any residual stress.

2.2. Swelling tests

The penetration of methanol in PMMA beads was measured in a sealed quartz cuvette at a temperature of ~25 °C and observed with a Wild M420 polarized light stereomicroscope equipped with a digital optical measuring accessory (Wild MMS235; accurate to ±0.001 mm). The schematic of a swelling PMMA bead system is shown in Fig. 1, where $a_o(0)$ is the initial radius of the bead, $a_o(t)$, the outer swollen radius of the bead at time t, and $a_i(t)$, the inner un-penetrated core radius of the bead at time t. Their corresponding diameters are represented by $d_o(0)$, $d_o(t)$ and $d_i(t)$, respectively (not shown in Fig. 1).

3. Results and discussion

3.1. Penetration kinetics

Typical methanol swelling and front penetration behavior in an annealed PMMA bead sample (cooled at 5 °C/min) are presented in Figs. 2–5. During methanol penetration, a sharp penetrating front in PMMA beads is generally visible as illustrated in Fig. 2. Fig. 3 shows the time dependence of such methanol front penetration measured with respect to the initial PMMA bead radius. In this case, after a characteristic induction period, the methanol penetrating front movement in PMMA bead appears to be linear in time over a major portion

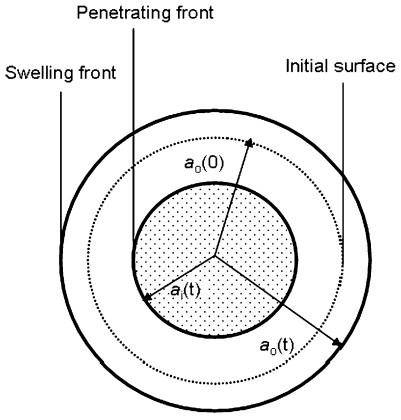

Fig. 1. Schematic of a swelling PMMA bead system.

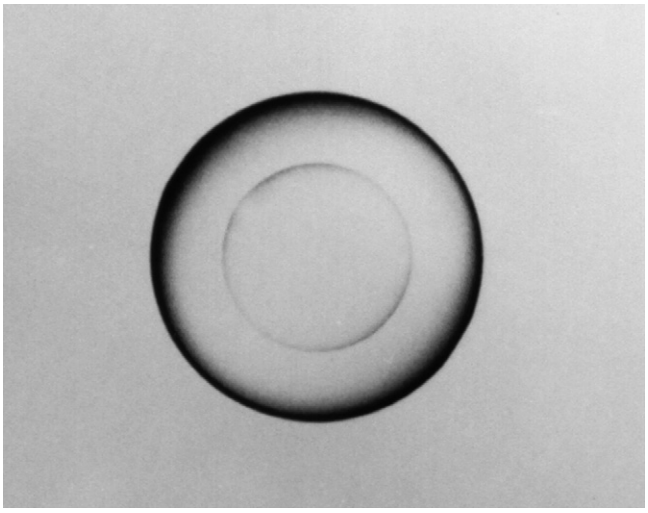

Fig. 2. Photomicrograph illustrating typical methanol front penetration in a PMMA bead.

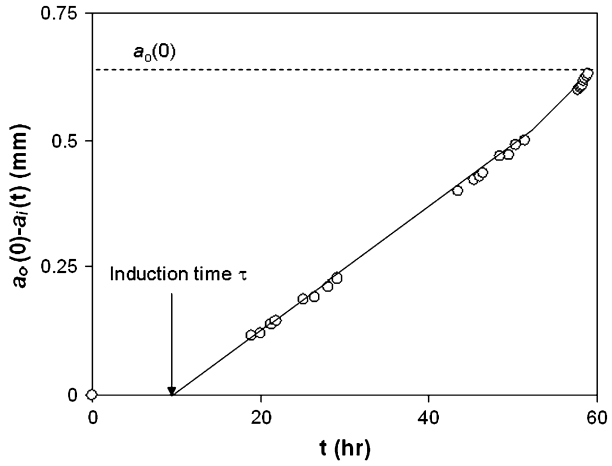

Fig. 3. Time dependence of methanol front penetration $[a_o(0) - a_i(t)]$ in a typical PMMA bead at 25 °C.

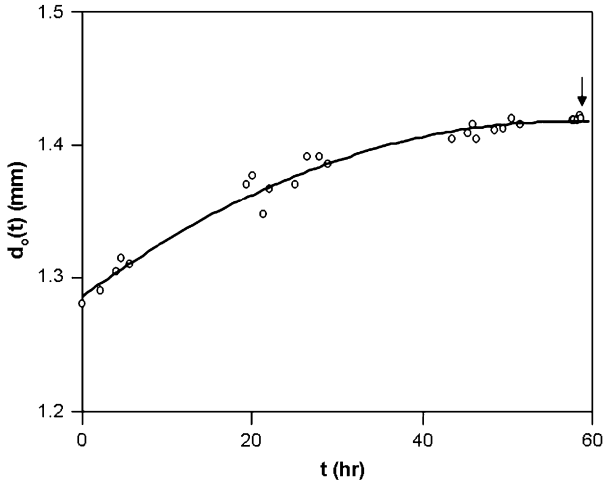

Fig. 4. Corresponding changes in outer diameter $d_o(t)$ during methanol front penetration in the PMMA bead sample of Fig. 3; ↓ solvent fronts meet.

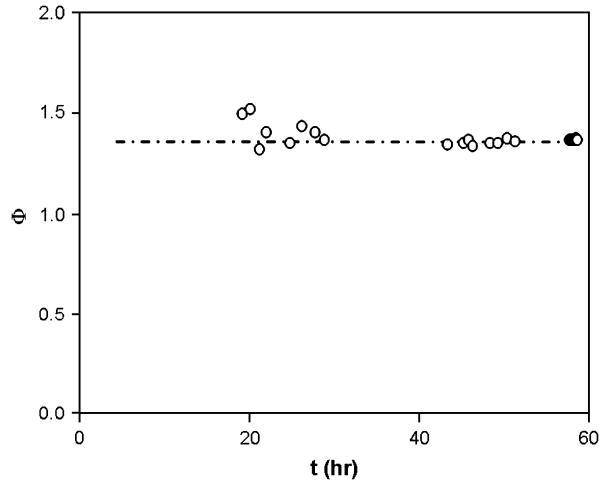

Fig. 5. Corresponding volume swelling ratio Φ in methanol penetrated region during methanol front penetration in the PMMA bead sample of Fig. 3.

(>70%) of the total penetration; the slope of which gives the solvent penetration rate ν. Beyond that, an apparent acceleration of the methanol front moving towards the core is evident. This acceleration of the penetrating front propagation has been shown to be a natural consequence of the spherical sample geometry [9]. Extrapolation of this linear front movement to zero front penetration gives the apparent induction time τ. It has been well established in our previous work [9,10] that the penetration of methanol in PMMA beads proceeds linear with time up to 60–70% of the total penetration before accelerating to the core and this extrapolated induction time agrees well with the experimentally estimated onset of methanol front movement.

The corresponding changes in the outer PMMA bead diameter, $d_o(t)$, as a function of contact time in methanol are shown in Fig. 4. Two distinctive features are worth noting here. Firstly, the PMMA bead diameter is seen to increase continuously right from the beginning prior to the appearance of a visible penetration front (compare with Fig. 3). This is attributed to the continuous penetration of the Fickian precursor of methanol in the surface region of the glassy PMMA sample during the induction period, prior to reaching a critical volume fraction of penetrant at the polymer surface [10]. Secondly, the PMMA bead diameter eventually reaches a plateau as soon as the penetrating methanol fronts have met at the center. This observation suggests the existence of a negligible concentration gradient behind the methanol swelling front. As shown in Fig. 5, the volume swelling ratio in methanol penetrated region, defined as $\Phi = (a_o^3(t) - a_i^3(t))/(a_o^3(0) - a_i^3(t))$, remains fairly constant over time once the penetrating front starts to propagate beyond the induction time. This reflects the fact that the methanol concentration in the swollen PMMA region is nearly constant and there is a negligible concentration gradient behind the methanol swelling front.

3.2. Effect of sample size

Fig. 6 summarizes the effect of PMMA bead diameter on the observed induction time τ leading to the development of

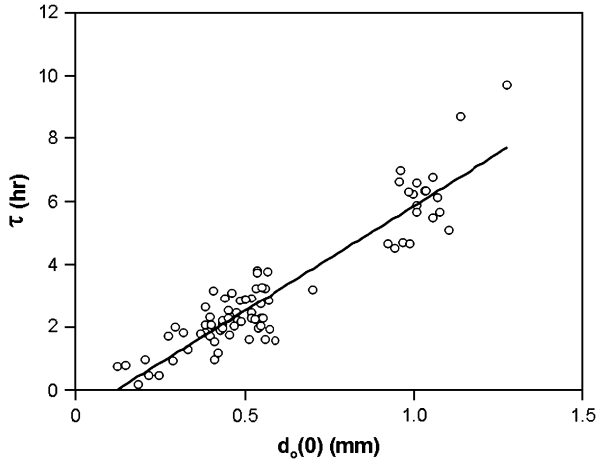

Fig. 6. Effect of PMMA bead diameter on the observed induction time τ prior to establishing the methanol penetration front at 25 °C.

methanol penetration front, based on the data collected on 80 individual PMMA bead samples (annealed at 130 °C, cooled at 5 °C/min). The corresponding methanol front penetration rate v as a function of the PMMA bead diameter is presented in Fig. 7. Contrary to the common notion that the induction time and front penetration rate are material constants, the results of Figs. 6 and 7 demonstrate clearly a dependence of induction time and front penetration rate on sample diameter. It is evident that the observed induction time generally increases, whereas the front penetration rate exhibits a weak decreasing trend, with increasing sample diameter. Such dependencies of induction time and front penetration rate on sample size are not predicted by existing theories of Case II diffusion.

According to Rossi et al. [8] and Astarita and Sarti [12], the diffusion flux into the glassy region during the induction period has an upper limit set by the product of the front penetration rate and the critical penetrant concentration, as dictated by the plasticization kinetics. Such phenomenological description is equivalent to the concept of surface mass transfer resistance. In fact, in treating the solvent front penetration

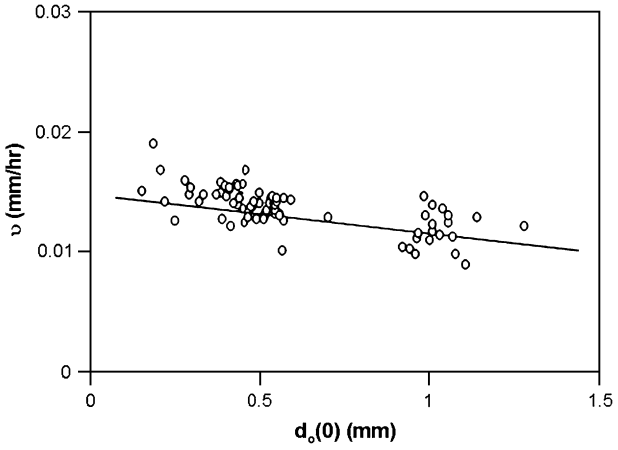

Fig. 7. Corresponding methanol front penetration rate v as a function of the diameter of PMMA bead samples of Fig. 6.

in glassy polymers as a moving boundary problem, Lee and Kim [9] have shown that the surface resistance boundary condition generally gives rise to a diffusion front moving nearly linear with time whenever the surface mass transfer resistance becomes significant. The relevance of such surface flux limited phenomenon in Case II diffusion has also been confirmed recently by McDonald et al. [13]. Unlike the semi-infinite medium assumption adopted by Rossi et al., the sample dimension in the direction of Case II solvent penetration is usually finite. By incorporating a similar upper limit of the surface flux as a boundary condition for the Fickian precursor of methanol in the surface region of a glassy polymer sample of finite dimension, it can be shown that the smaller the sample dimension the less time it takes for the polymer bead surface to reach a critical solvent concentration necessary for establishing the moving front, especially for relatively small samples (e.g., <1 mm dia.) [14]. Therefore, larger PMMA beads will require longer induction time to establish the moving front.

Additionally, the observed sample size dependency may also be related to stress effect since the swelling surface region will develop a compressive stress due to the constraint of the underlying rigid glassy core. This stress arises as a result of the penetration of the Fickian precursor of methanol in the surface region of the PMMA bead producing a continuous increase in sample diameter during the induction period due to volume swelling (see Fig. 4). This is analogous to the case of a swollen shell bonded by a rigid glassy core. The stress evolution in such a system in cylindrical and spherical geometries has been analyzed by Treloar [15] and Klier and Peppas [16], respectively. According to these analyses, a compressive stress distribution, with an associated distribution in polymer volume fraction, exists in the surface region of the swollen shell as a consequence of the inhomogeneous swelling in spherical and cylindrical samples with glassy cores. Furthermore, its magnitude is greatly affected by the ratio of the radius of the underlying rigid glassy core to the initial radius of the glassy core prior to swelling, with a higher surface compressive stress occurring when this ratio is closer to 1. In other words, with a given thickness of the surface swelling region, the larger the bead size the larger the compressive stress at the surface. Since applied compressive stress has been shown by More et al. [17] to increase the Case II induction time and decrease the methanol front penetration rate in PMMA sheet samples, it is reasonable to expect that this swelling induced compressive stress at the surface region may also contribute to the observed Case II diffusion behavior in PMMA bead samples. In particular, in the sample size range studied here, the larger the bead diameter the longer the induction time and the smaller the penetration rate due to the presence of a higher compressive stress in the swelling surface region.

The above considerations suggest that the observed size effect on induction time comes from both the surface flux and the surface stress effects whereas the observed size effect on penetration rate is only linked to the stress effect. Judging from the observed weak dependence of methanol front penetration rate on PMMA sample diameter (varying less than a factor of 2 in the diameter range studied; Fig. 7), it is quite

reasonable that the induction time dependence on sample diameter due to the stress effect may be similarly weak. Therefore, the more pronounced induction time dependence on sample diameter observed here (varying up to a factor of 20 or more; Fig. 6) is most likely resulted from the surface flux effect.

4. Conclusion

The characteristic Case II solvent front penetration behavior in a methanol–PMMA bead system has been studied at 25 °C in the particle diameter range of 0.125–1.280 mm. The observed induction time generally increases, whereas the front penetration rate exhibits a weak decreasing trend, with increasing sample diameter. Such dependencies of induction time and front penetration rate on sample size, although not predicted by existing theories of Case II diffusion, have been attributed to the size-dependent nature of several physical processes originated from the Fickian precursor penetrating ahead of the moving solvent front in an inhomogeneous swelling system of finite dimension. Therefore, based on surface flux considerations, it is clear that the smaller the sample dimension the shorter time it takes to reach the critical surface concentration needed to establish the moving front, especially for relatively small samples (e.g., <1 mm dia. as in the present study). In other words, larger PMMA beads will require longer induction time to establish the moving front. On the other hand, based on stress evolution considerations, a compressive stress distribution exists in the surface region of the spherical PMMA bead sample as a consequence of the inhomogeneous swelling process, and the larger the bead diameter the higher the compressive stress in the swelling surface region. Given the fact that applied compressive stress has previously been shown to increase Case II induction time and decrease methanol front penetration rate in sheet PMMA samples, it is reasonable to expect that this swelling induced compressive stress at the surface region may also contribute to the Case II diffusion behavior in PMMA beads described here. However, since the dependence of the observed front penetration rate (and hence the induction time) on sample diameter due to surface stress effect appears to be generally weak, the observed more pronounced induction time dependence on sample diameter is most likely related to the surface flux effect.

References

[1] Alfrey T, Gurnee EF, Lloyde WG. J Polym Sci 1966;C12:249–61.
[2] Thomas NL, Windle AH. Polymer 1978;19:255–65.
[3] Thomas NL, Windle AH. Polymer 1981;22:627–38.
[4] Thomas NL, Windle AH. Polymer 1982;23:529–42.
[5] Hui CY, Wu KC, Lasky RC, Kramer EJ. J Appl Phys 1987;61:5129–36.
[6] Hui CY, Wu KC, Lasky RC, Kramer EJ. J Appl Phys 1987;61:5137–49.
[7] Lasky RC, Kramer EJ, Hui CY. Polymer 1988;29:673–9.
[8] Rossi G, Pincus PA, De Gennes PG. Europhys Lett 1995;32:391–6.
[9] Lee PI, Kim CJ. J Membr Sci 1992;65:77–92.
[10] Lee PI. Polymer 1993;34:2397–400.
[11] Qian T, Taylor PL. Polymer 2000;41:7159–63.
[12] Astarita G, Sarti GC. Polym Eng Sci 1978;18:319–95.
[13] McDonald PJ, Godward J, Sackin R, Sear RP. Macromolecules 2001;34:1048–57.
[14] Li JX, Lee PI. Prediction of particle size effect on Case II diffusion in glassy polymers. In preparation.
[15] Treloar LRG. Polymer 1976;17:142–6.
[16] Klier J, Peppas NA. Polymer 1987;28:1851–9.
[17] More AP, Donald AM, Henderson A. Polymer 1992;17:3759–61.